

On the Constant Depth Implementation of Pauli Exponentials

Ioana Moffic* and Alexandru Paler†
Aalto University, Espoo, Finland

We decompose for the first time, under the very restrictive linear nearest-neighbour connectivity, $Z \otimes Z \dots \otimes Z$ exponentials of arbitrary length into circuits of constant depth using $\mathcal{O}(n)$ ancillae and two-body XX and ZZ interactions. Consequently, a similar method works for arbitrary Pauli exponentials. We prove the correctness of our approach, after introducing novel rewrite rules for circuits which benefit from qubit recycling. The decomposition has a wide variety of applications ranging from the efficient implementation of fault-tolerant lattice surgery computations, to expressing arbitrary stabilizer circuits via two-body interactions only, parallel decoding of quantum error-correcting computations and to reducing the depth of NISQ computations, such as VQE.

I. INTRODUCTION

The efficient compilation of Pauli exponentials has far-reaching implications in quantum computing. Whenever the exponentiation angle is $\pi/2$, Pauli strings can be used as measurement operators for stabilizing quantum systems (e.g. [1–3]). When the angle is part of the set $[\pi/2, \pi/4, \pi/8]$, the exponentiated Pauli strings can be interpreted as multi-body measurements which implement fault-tolerant, lattice surgery computations [4–6]. In the case of arbitrary rotation angles, these strings are central to VQE-algorithms (e.g. [7]) and to the form of UCCSD terms in quantum chemistry [8]. Pauli exponentials are phased gadgets in the ZX-calculus [9].

We introduce a novel decomposition of Pauli exponentials, which uses a linear number of ancillas (effectively doubling the number of qubits) and only two-body XX and ZZ interactions. Two-body interactions are the easiest to engineer and implement, and are native to Majorana computers [2], ion traps [10], silicon spin qubits [11], as well as to fault-tolerant and error-correction circuits. In other words, we present a very efficient way of emulating the all-to-all connectivity (on linear nearest-neighbour architectures) required for executing exponentiated Pauli strings.

Increased interest is being expressed in finding time-optimal algorithms for calculating Pauli decompositions of arbitrary complex matrices [12] and in designing optimal compilers for arbitrary Pauli operators [13]. Our method complements these efforts, by providing a way to efficiently execute any Pauli string exponential via two-body XX and ZZ interactions, even under the constraints of nearest-neighbour topologies. To the best of our knowledge, our constant depth implementation is the most efficient known decomposition of such strings, and has the advantage of significantly lowering the cost of implementing arbitrary computations.

In the following, we discuss the novelty of our method and introduce the building blocks of our derivation in

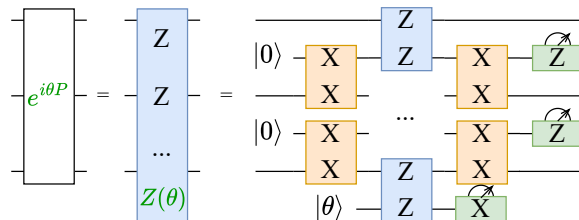


FIG. 1. An n -qubit Pauli exponential is decomposed into a constant depth sequence of XX and ZZ interactions and $\mathcal{O}(n)$ ancillae. We use the shorthand notation $e^{i\theta P} = P(\theta)$, and consider that P is formed exclusively of Z terms: $P = Z \otimes Z \dots \otimes Z$. A general string can always be decomposed into single-qubit Clifford gates conjugating the Z -terms of P [9]. In this figure, we assume that θ is arbitrary, such that our construction is extending P with an additional Z term (marked green) and an ancilla initialized in $|\theta\rangle = Rz(\theta)|+\rangle$ [4].

the Methods section. We also briefly describe the wide applicability of our decomposition in the Applications section. The correctness of our method, as well as the complete proof of the decomposition from Fig 1 can be found in Figs 8, 9, 10,

A. Novelty

The constant-depth execution of Pauli exponentials was previously achievable, however, emulating all-to-all connectivity incurred substantial costs. For NISQ machines the costs are, for example, either quadratic qubit overheads and complex four-body interactions [14], the shuttling time in ion trap and neutral atom computers, or the number of SWAP gates in superconducting chips. In error-corrected machines, the costs arise from the difficulty of engineering the surface code buses, which facilitate long-range interactions (e.g. [15]). Other costs come in the form of resource intensive layouts of logical qubits (e.g. [4, 16]), or even complex decoding strategies (e.g. [17]).

Without being generalized to arbitrary rotation angles

* ioana.moffic@aalto.fi

† alexandru.paler@aalto.fi

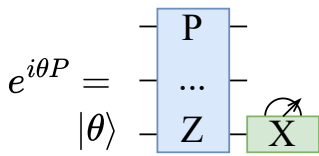


FIG. 2. The **ROT** rewrite rule implements the exponential of the Pauli P by introducing an ancilla initialized in $|\theta\rangle = Rz(\theta)|+\rangle$, extending the Pauli string with a Z -term for the ancilla, and measuring the ancilla in the X -basis[4].

or number of qubits, constructions similar to ours appeared in [2, 3]. Those constructions were derived and verified by applying the ZX-calculus on smaller-scale diagrams. In contrast, we introduce novel circuit rewrite rules, derive and show the correctness of our decomposition using circuit diagrams. We could have used ZX [18] for illustrating the correctness of the derivation from Fig. 8 through spider fusions and strong complementarity, however we discovered the **FUSE** rule by circuit rewrites, thus it felt more natural to us to stay in the realm of quantum circuits.

Our decomposition is applicable to both NISQ and error-corrected machines. In contrast, a result concerning long range CNOTs has been proposed by [19]. Their adaptive circuit construction uses the same number of ancillae as our decomposition. Nevertheless, due to the exclusive focus on CNOT gates, their construction is only suitable for NISQ computers. Another constant-depth implementation of long range CNOTs using pairwise measurements is presented in [16], and is motivated by the fact that efficient decompositions of Pauli exponentials were not known at the time. Our work bridges the gap that motivated [16].

II. METHODS

The string P can be exponentiated to a unitary by computing $e^{i\theta P}$. We consider the measurement-based implementation of the exponentiated Pauli strings [4], such that, in practice, the implementation uses *an additional Z term in the Pauli string* (green in Fig. 1) and an ancilla rotated by θ . Consequently, $e^{i\theta P}$ is achieved by the rule **ROT** from Fig. 2.

The lhs. of Fig. 1 represents the unitary obtained by the exponentiation. The rhs. is the decomposition which includes ancillae for enabling the XX interactions, as well as the $|\theta\rangle$ ancilla initialized for performing a teleportation-based gate.

A. Measurement-based implementation

When implementing the Pauli exponentials on fault-tolerant machines, the θ rotation is first decomposed into a sequence of rotation gates supported by the QEC. This

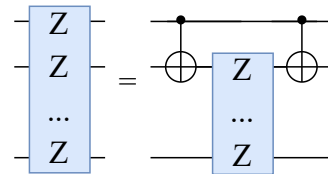


FIG. 3. The **PG** rewrite takes an n -qubit string and decomposes it into a $(n - 1)$ -qubit string and two CNOTs.

increases the depth proportionally to the length of the gate sequence. Moreover, the depth will additionally increase by a constant factor, as each rotation is probabilistic and might require corrections [4] (e.g. if the X -measurement results in the -1 eigenvalue, then a corrective rotation of 2θ is needed). Corrections can be tracked in a Pauli frame, when the angles correspond to Pauli gates.

Moreover, we assume that the two-body interactions are also measurement-based. The latter will introduce corrective terms (e.g. [3]), but the corrections can be tracked in a Pauli frame, as the underlying circuit will consist solely of CNOT gates and ancillae initialised or measured in a discrete set of rotated basis [20, 21].

If the exponentials are implemented on NISQ machines, the θ rotation is a single qubit gate. The corrective terms generated by the measurements of the ancillae will be applied adaptively without increasing the depth of the circuit [19].

As a conclusion, in all the following diagrams we omit the corrective terms introduced by the measurements. Corrections can be tracked through the circuit, or can be applied immediately after the exponentiated Pauli without affecting the depth of the decomposition.

B. Decomposing the Pauli exponentials

We use the graphical calculus of quantum circuits for reasoning about the decomposition of the Pauli exponentials. To this end, we first present the rewrite rules used to obtain the generalized decomposition from Fig. 1. The result from Fig. 1 is obtained by applying the following algorithm:

1. *Input*: arbitrary Pauli exponential P with angle θ ;
2. Apply **ROT**, if θ is not $\pi/2$ – this extends the Pauli string by an additional Z term and the circuit will include the $|\theta\rangle$ ancilla; if the angle is $\pi/2$ the Pauli string is left unchanged and $|\theta\rangle$ is not appended;
3. Repeat the sequence of rewrite rules **PG**, **LS**, **MR**, **FUSE**, until the largest Pauli string acts on a maximum of two qubits.

We start by decomposing an arbitrary Pauli string P into a string $C = C_0 \otimes \dots \otimes C_n$ of single qubit Clif-

ford gates C_i , and a string $P_z = Z \otimes \dots \otimes Z$, such that $P = CP_zC^\dagger$. As an example, single qubit gates can be efficiently implemented in practice [22, 23] in surface codes. We continue by decomposing P_z via the **PG** rule [9] (Fig. 3). CNOTs are expressed in lattice surgery style[24] decompositions (Fig. 4). After using **PG**, we choose the first **LS** rewrite for the lhs. CNOT, and the second rewrite for the rhs. CNOT.

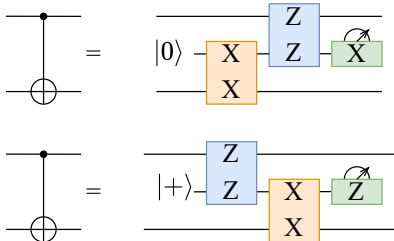


FIG. 4. The **LS** rewrite can decompose a CNOT into any of the two functionally equivalent forms. A CNOT will require an ancilla, one XX and one ZZ two-body interaction. The figure does not include the corrective terms.

We replace a sequence of measurement and reset operations in the same basis with an equivalent measurement-based implementation by using the **MR** rule (Fig. 5). This is, to the best of our knowledge, a novel quantum circuit rewrite rule. The rule is the inverse of the copy rule from the ZX-calculus [25].

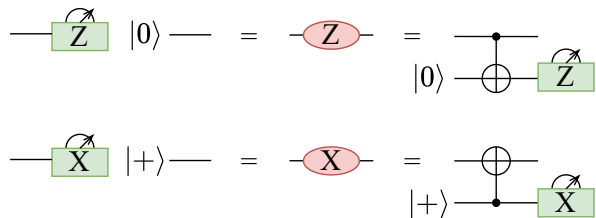


FIG. 5. The **MR** rewrite is joining a measurement and a reset in the same basis into an operation represented by the oval element (e.g. Z). Instead of explicitly measuring and resetting, we will consider the circuits on the rhs for achieving this task. The figure does not include the corrective terms.

The **MR** rewrite rule is applicable for the optimization of circuits which benefit from qubit recycling schemes[26, 27]. By merging the measurement and the reset, it is possible to commute gates across seemingly disjoint parts of the circuit. This has the potential to generate novel optimization heuristics. In particular, this approach has enabled us to derive the **FUSE** rule (Fig. 6): we can merge two-body interactions into a single one, if a measure-and-reset acts on one of the qubits between them.

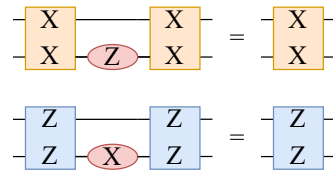


FIG. 6. The **FUSE** reduces the depth of the decomposition by absorbing an oval X or Z element.

III. APPLICATIONS

Two-body interactions such as XX and ZZ are commonly used in a wide variety of quantum computations and architectures. Herein, we list a few of the applications enabled by our novel approach.

A. Lattice Surgery

Lattice surgery is the de facto standard way of implementing computations with QLDPC codes [6], such as the surface code. Therein, the logical qubits of the circuits are arranged on a 2D layout of patches (e.g. Fig. 7), and ancillary space between the patches supports long range multi-body measurements. The latter are expressed as generalized Pauli exponentials. The structure of the layout plays a significant role in the trade-off between a computation's speed and the required amount of physical hardware [4, 28]. Although our decomposition uses ancillae, these are readily available in most of the lattice surgery layouts considered for compiling fault-tolerant computations.

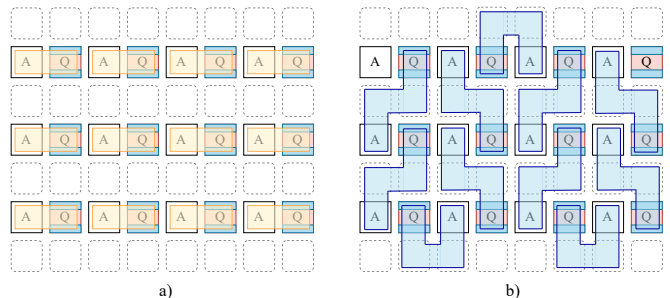


FIG. 7. Multi-body $Z \otimes \dots \otimes Z$ interaction implemented by lattice surgery. The patch layout is adapted from [28]: pink patches (Q) are holding logical qubits, and gray patches (A) are ancilla for XX and ZZ interactions. The blue boundaries are the Z operators of the logical A patches. a) according to Fig. 1, we initialize two ancilla in $|0\rangle$ and perform XX two-body interactions (orange) with the Q patches; c) afterwards we perform pairwise ZZ two-body interactions (blue) between pairs of Q and A patches. Finally, the interactions from a) are repeated. The interaction schedule from a) and b) is highly regular and can be further optimized in terms of hardware overheads.

The general compilation strategy for lattice surgery is to first decompose arbitrary algorithms into generalized Pauli exponentials [4], and then to implement these exponentials via multi-body measurements. This approach has multiple disadvantages.

The resulting Pauli exponentials become very long-range and cover large portions of the layout. This hinders the parallelisation of the operations, and alternative compilation methods have been proposed to overcome this, such as [16] (shows how to perform a constant depth CNOT using two-body measurements), and [29], which compiles to Clifford+T instead of exponentiated Paulis.

Our approach is directly applicable to the compilation method from [4] – we do not require compiling to CNOTs and then decomposing them to irregular XX and ZZ measurement patterns. The advantage of our decomposition is the very regular measurement schedule (Fig. 7), which might enable high degrees of parallelism and massive optimizations when considering **FUSE**.

B. Parallel Decoding

Our decomposition enables the parallelisation of decoding by setting an upper bound on the maximum (equivalent) decodable distance that a QEC decoder will need to handle within one QEC cycle. In the following, we introduce the concept of equivalent decodable distance and restrict the discussion, without loss of generality, to rotated surface codes operated by lattice surgery.

An additional disadvantage of long-range Pauli exponentials is the large number of physical qubits (data and syndrome) that need to be decoded. For distance d , a surface code patch will require $2d^2 - 1$ physical qubits (data and syndrome). The decoding time scales with the size of the surface code patch. Usually, the decoding time is upper bounded by a low-degree polynomial, however, in practice it is still challenging to decode distances larger than 21 within the cycle time of the surface code.

In general, the lattice surgery merge operation between two surface code patches will cover $q = (m + 1)(2d^2 - 1)$ qubits, where m is the Manhattan distance between the patches. Decoding the long-range interaction is equivalent to decoding a single patch of distance approximately

$$\sqrt{\frac{q}{2(m+1)}}.$$

As an example, merging two neighboring patches of distance 21 will yield a patch covering $2 \times 881 = 1762$ qubits. This is roughly equivalent to a distance 29 patch. If the patches are separated by a single logical patch of distance 21, the equivalent decoding distance would be 36.

In practice, decoding is very challenging. The computational complexity of the decoding algorithms scales polynomially (more than linear) [30], and surface code compilers do not guarantee short-range implementations of Pauli exponentials. Assuming a logical computation of 100 logical qubits, a compact, resource efficient layout of

surface code patches would consist of approximately 150 patches[4]. The average Manhattan distance between two arbitrary patches would be around 25, and the average equivalent decoding distance would be 105. For an instance of Shor’s algorithm with 2048 logical qubits, the best-case equivalent decoding distance would be around 200. For a decoder with cubic runtime complexity [30], this would have an $\approx (10^2)^3 = 10^6$ increase in decoding time compared to decoding distance 21.

Our decomposition sets an upper bound on the equivalent decoding distance of arbitrary Pauli exponentials implemented via lattice surgery. For example, in Fig. 7 the blue interactions always cover only four patches. Assuming the distance of the patches is 21, the maximum equivalent decoding distance to decode would be 42.

At the same time, as seen in Fig. 7, all blue patches can be decoded in parallel. Our parallelisation method is reminiscent of the proposal from [31] (fixing the number of physical qubits per decoder) and the constructions from [32, 33] (decoders which communicate messages). For the latter, the decoders will communicate the observed correlated logical errors [17] after the long-range interaction is split via lattice surgery.

We conjecture that our decomposition, together with the methods from [17, 31, 32] will lead to the same decoding performance for Pauli exponentials of arbitrary length. Future work will focus on this analysis.

C. Constant Depth Fault-Tolerant Protocols

Recently, there has been an increased interest in using only two-body interactions to implement error correction (e.g. [2, 3]). Two-body interactions are preferred as quantum computers have limited connectivity between the qubits, and very often the connectivity is not long range (e.g. [19]).

From the perspective of stabilizer QECC codes, our decomposition allows any set of QECC stabilizers to be implemented in constant depth using pairwise XX and ZZ measurements. QECC code conversion schemes [34] can also be implemented locally using pairwise interactions. Additionally, after carefully choosing the pairwise interaction schedules, our method might lead to results similar to the ones from [35]. Our decomposition involves only two-body measurements and may find relevance to subsystem codes such as the Bacon-Shor code [36] or its Floquet version [35].

Our method is also useful for the implementation of Clifford circuits in constant depth by using only pairwise interactions. For example, the authors of [37] show a way of implementing Clifford circuits fault-tolerantly in constant depth via non-local, multi-qubit Pauli operator measurements. We achieve a local implementation of the circuits at the cost of doubling the number of qubits.

It should be noted that the listed constructions might not be fully fault-tolerant, e.g. introduce hook errors in certain scenarios, and such analysis is left for future work.

D. NISQ computations

The recursive decomposition of Pauli exponentials (i.e. phase gadgets) using **PG** will result in a ladder of CNOTs. These ladders are frequently encountered in the circuits expressing UCCSD terms. The long range CNOT construction from [19] has already recognized that such terms can be implemented in constant depth.

Our decomposition achieves the same constant depth, but this time using two-body interactions. In conjunction with architectures such as [11], our decomposition can offer speed-ups to the execution of adaptive VQE [7] or other QAOA-like algorithms.

IV. GENERALIZATION

So far, we considered constant depth decompositions of Pauli strings of the form $Z \otimes \dots \otimes Z$. Nevertheless, there might be qubits which are not involved in the operation, and the corresponding Pauli string will include an I term for those qubits.

Without loss of generality, we discuss the constant depth, nearest-neighbour implementation of exponentials of the form $Z \otimes \dots \otimes I \dots \otimes Z$ – a single Z at the start and the end of the string and at least one I in between.

Considering the circuit from Fig. 1, the challenge is to *jump* over the qubits which should not be operated by Z operators – these qubits are left unchanged by the I . In the following, we consider the position (index) of the Z operators in the string (*first*, *last*), such that the discussion will revolve around storage and layouts.

One solution is to permute the qubits such that all I terms are moved to the end on the Pauli string. For example, $Z \otimes \dots \otimes I \dots \otimes Z$ will be implemented via a single two-body nearest-neighbour interaction $Z \otimes Z \dots \otimes I$. However, sorting introduces two SWAP networks (one before the Pauli string exponential, and another one afterwards) of logarithmic depth (e.g. [9]) instead of a constant depth.

Another solution is to use qudits (moving the qubit state into a higher dimension in order to protect it from qubit Z gates) or special layouts which enable the constant depth construction of Bell pairs using the method from [16].

A. Qudits

It is possible, but not necessarily practical with the current generation of quantum computers, to embed the qubit computation into a system of qudits. To this end, we choose ququarts whose states are spanned by the following basis states: $|0\rangle$, $|1\rangle$, $|2\rangle$, $|3\rangle$. We will assume that all the wires are ququarts instead of qubits.

We make the observation that qubit gates can be applied on qudits [38] and that whenever this happens, the

higher levels of the ququart are left unchanged. For example, the qubit Z_2 gate (the subscript indicates the dimension of the qudit, e.g. two is for qubits, and four for ququarts) can be embedded into a 4×4 matrix written in block form as $Z_4 = \begin{pmatrix} Z_2 & 0 \\ 0 & I_2 \end{pmatrix}$.

At this stage, whenever we want to apply a qubit operator I_2 , we can now move the qubit state two levels higher with the ququart X_4 gate [39] which acts as $X_4|i\rangle = |(i+1)\%4\rangle$, such that $X_4^2(a|0\rangle + b|1\rangle) = a|2\rangle + b|3\rangle$. By assuming I_2 embedded into I_4 , we can write the following (as our Z_4 gate leaves the higher states unchanged):

$$I_2(a|0\rangle + b|1\rangle) = X_4^2 Z_4 X_4^2 (a|0\rangle + b|1\rangle)$$

Therefore, whenever ququarts and the X_4 and Z_4 gates are supported, we can implement the qubit $Z \otimes \dots \otimes I \dots \otimes Z$ Pauli string by replacing each I with the single ququart $X_4^2 Z_4 X_4^2$. The result is a continuous string of qubit Z operators which can be implemented according to the decomposition from Fig. 1.

An alternative to using ququarts is to use one additional qubit q placed next to each ancilla a from Fig. 1. These q qubits will be initialized in $|0\rangle$, and the I operators from the Pauli string would be replaced by $SWAP(a, q)$, a Z on a , followed by $SWAP(a, q)$. This construction would not be nearest-neighbour, but next-nearest neighbour.

B. The qubit layout

The nearest-neighbour implementation of the two-body interaction is only possible if the qubit layout supports it. For example, in Fig. 7 it is not possible to implement the blue merge operations between nearest-neighbour patches, because each logical Q-patch is surrounded by one ancilla A-patch and three routing patches (not marked by any letter).

In a *linear* nearest neighbour layout of qubits, the logical qubits are arranged in a line similar to $Q \ 0 \ Q \ 0 \dots \ Q$, where 0 are ancillae initialized in $|0\rangle$. In this scenario, pairwise nearest-neighbour interactions are not possible without resorting to ququarts, as discussed in the previous section. Consequently, the long range construction from [19] uses nearest-neighbour pairwise interactions, but it uses the less general layout $Q \ 0 \ 0 \ 0 \dots \ Q$, where all the qubits between the first and last one are initialized in $|0\rangle$.

A *bi-linear* nearest neighbour layout of qubits of the form $\begin{matrix} Q & 0 & Q & 0 & \dots & Q \\ r & r & r & r & \dots & r \end{matrix}$ allows for *jumping* over qubits operated by I and maintaining the nearest-neighbour decomposition – the routing qubits r can be used first to prepare Bell pairs using the constant depth recipe from [16]. The layout from Fig. 7 has the same properties the bi-linear nearest neighbour layout has.

V. CONCLUSION

We introduced a novel and very space-time efficient decomposition of Pauli exponentials. Compared to previous methods of implementing long range interactions (e.g. LHZ [14]) our method uses only local two-body interactions, has a linear qubit cost (versus quadratic qubit costs, or time intensive shuttling or SWAP gate schedules) and is applicable to a very wide range of quantum computations, from NISQ to the automatic Floquetification of QEC codes. Our approach is also enabling the parallelisation and message passing distribution of QEC decoders. Future work will focus on a more detailed analysis of mentioned applications.

VI. ACKNOWLEDGMENTS

We thank Alexander Cowtan, Matthew Steinberg, M. Sohaib Alam, György Gehér for the stimulating dis-

cussions, Arshpreet Singh Maan and Huyen Do for their feedback, Ryan Babbush for suggesting the application to Adapt-VQE and the Centro de Ciencias de Benasque Pedro Pascual for hosting us while preparing the manuscript. This research was developed in part with funding from the Defense Advanced Research Projects Agency [under the Quantum Benchmarking (QB) program under award no. HR00112230006 and HR001121S0026 contracts], and was supported by the QuantERA grant EQUIP through the Academy of Finland, decision number 352188. The views, opinions and/or findings expressed are those of the author(s) and should not be interpreted as representing the official views or policies of the Department of Defense or the U.S. Government.

-
- [1] J. Roffe, D. Headley, N. Chancellor, D. Horsman, and V. Kendon, Protecting quantum memories using coherent parity check codes, *Quantum Science and Technology* **3**, 035010 (2018).
- [2] L. Grans-Samuelsson, R. V. Mishmash, D. Aasen, C. Knapp, B. Bauer, B. Lackey, M. P. da Silva, and P. Bonderson, Improved pairwise measurement-based surface code, *Quantum* **8**, 1429 (2024).
- [3] C. Gidney, A pair measurement surface code on pentagons, *Quantum* **7**, 1156 (2023).
- [4] D. Litinski, A game of surface codes: Large-scale quantum computing with lattice surgery, *Quantum* **3**, 128 (2019).
- [5] G. Watkins, H. M. Nguyen, K. Watkins, S. Pearce, H.-K. Lau, and A. Paler, A high performance compiler for very large scale surface code computations, *Quantum* **8**, 1354 (2024).
- [6] A. Cowtan, Ssip: automated surgery with quantum ldpc codes, arXiv preprint arXiv:2407.09423 (2024).
- [7] H. R. Grimsley, S. E. Economou, E. Barnes, and N. J. Mayhall, An adaptive variational algorithm for exact molecular simulations on a quantum computer, *Nature communications* **10**, 3007 (2019).
- [8] P. K. Barkoutsos, J. F. Gonthier, I. Sokolov, N. Moll, G. Salis, A. Fuhrer, M. Ganzhorn, D. J. Egger, M. Troyer, A. Mezzacapo, *et al.*, Quantum algorithms for electronic structure calculations: Particle-hole hamiltonian and optimized wave-function expansions, *Physical Review A* **98**, 022322 (2018).
- [9] A. Cowtan, S. Dilkes, R. Duncan, W. Simmons, and S. Sivarajah, Phase gadget synthesis for shallow circuits, in *16th International Conference on Quantum Physics and Logic 2019* (Open Publishing Association, 2019) pp. 213–228.
- [10] S. Debnath, N. M. Linke, C. Figgatt, K. A. Landsman, K. Wright, and C. Monroe, Demonstration of a small programmable quantum computer with atomic qubits, *Nature* **536**, 63–66 (2016).
- [11] G. Üstün, A. Morello, and S. Devitt, Single-step parity check gate set for quantum error correction, *Quantum Science and Technology* **9**, 035037 (2024).
- [12] T. N. Georges, B. K. Berntson, C. Sünderhauf, and A. V. Ivanov, Pauli decomposition via the fast walsh-hadamard transform (2024), arXiv:2408.06206 [quant-ph].
- [13] I. D. Smith, M. Cautrès, D. T. Stephen, and H. P. Nautrup, Optimally generating $\mathfrak{su}(2^n)$ using pauli strings (2024), arXiv:2408.03294 [quant-ph].
- [14] W. Lechner, P. Hauke, and P. Zoller, A quantum annealing architecture with all-to-all connectivity from local interactions, *Science advances* **1**, e1500838 (2015).
- [15] S. Saadatmand, T. L. Wilson, M. Field, M. K. Vijayan, T. P. Le, J. Ruh, A. S. Maan, I. Moflic, A. Caesura, A. Paler, *et al.*, Fault-tolerant resource estimation using graph-state compilation on a modular superconducting architecture, arXiv preprint arXiv:2406.06015 (2024).
- [16] M. Beverland, V. Kliuchnikov, and E. Schoute, Surface code compilation via edge-disjoint paths, *PRX Quantum* **3**, 020342 (2022).
- [17] M. Cain, C. Zhao, H. Zhou, N. Meister, J. Ataiades, A. Jaffe, D. Bluvstein, and M. D. Lukin, Correlated decoding of logical algorithms with transversal gates, arXiv preprint arXiv:2403.03272 (2024).
- [18] N. de Beaudrap, A. Kissinger, and J. van de Wetering, Circuit extraction for zx-diagrams can be #p-hard, in *49th International Colloquium on Automata, Languages, and Programming (ICALP 2022)* (Schloss-Dagstuhl-Leibniz Zentrum für Informatik, 2022).
- [19] E. Bäumer and S. Woerner, Measurement-based long-range entangling gates in constant depth, arXiv preprint arXiv:2408.03064 (2024).
- [20] A. Paler, I. Polian, K. Nemoto, and S. J. Devitt, Fault-tolerant, high-level quantum circuits: form, compilation and description, *Quantum Science and Technology* **2**, 025003 (2017).

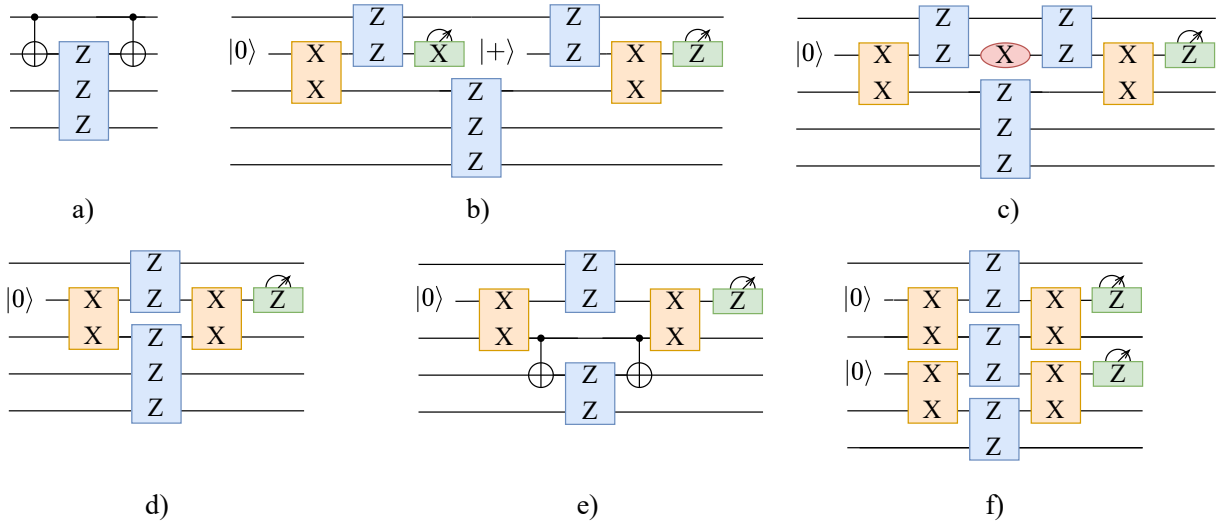


FIG. 8. Correctness of the generalized decomposition, illustrated by an example of decomposing a Pauli string of four Z terms: a) applying the **PG** rule; b) decomposing the two CNOTs using **LS**; c) the X-measurement and the initialization in $|+\rangle$ can be merged using **MR** into a red oval X element; d) the two ZZ parities surrounding the red oval are fused using **FUSE**; e) **PG** is applied again and inserts two CNOTs; f) the CNOTs are decomposed with **LS**, the measure and reset are merged with **MR** and, finally, **FUSE** is applied.

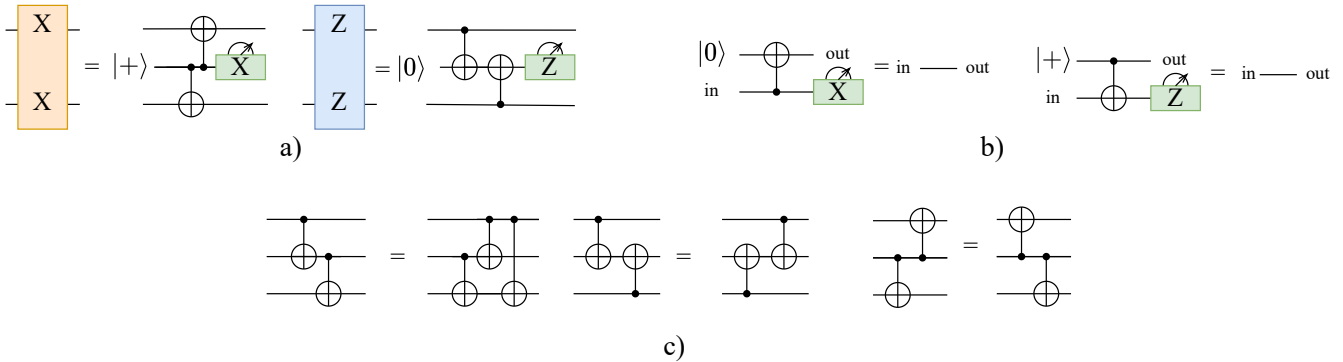


FIG. 9. Rewrite rules used as building blocks for more complex circuit identities (the figure does not include the corrective terms): a) the **XXC** and **ZZC** are circuit decompositions for the two-body XX and ZZ interactions; b) **REMZ** and **REMX** are replacing teleportation-like sub-circuits with the identity; c) **CNOT** commutation rules.

- [21] M. K. Vijayan, A. Paler, J. Gavriel, C. R. Myers, P. P. Rohde, and S. J. Devitt, Compilation of algorithm-specific graph states for quantum circuits, *Quantum Science and Technology* **9**, 025005 (2024).
- [22] G. P. Gehér, C. McLauchlan, E. T. Campbell, A. E. Moylett, and O. Crawford, Error-corrected hadamard gate simulated at the circuit level, *Quantum* **8**, 1394 (2024).
- [23] C. Gidney, Inplace access to the surface code y basis, *Quantum* **8**, 1310 (2024).
- [24] D. Horsman, A. G. Fowler, S. Devitt, and R. Van Meter, Surface code quantum computing by lattice surgery, *New Journal of Physics* **14**, 123011 (2012).
- [25] J. van de Wetering, Zx-calculus for the working quantum computer scientist, arXiv preprint arXiv:2012.13966 (2020).
- [26] A. Paler, R. Wille, and S. J. Devitt, Wire recycling for quantum circuit optimization, *Physical Review A* **94**, 042337 (2016).
- [27] H. Jiang, Qubit recycling revisited, *Proceedings of the ACM on Programming Languages* **8**, 1264 (2024).
- [28] L. Lao, B. van Wee, I. Ashraf, J. Van Someren, N. Khammassi, K. Bertels, and C. G. Almudever, Mapping of lattice surgery-based quantum circuits on surface code architectures, *Quantum Science and Technology* **4**, 015005 (2018).
- [29] T. LeBlond, C. Dean, G. Watkins, and R. S. Bennink, Realistic cost to execute practical quantum circuits using direct clifford+ t lattice surgery compilation, arXiv preprint arXiv:2311.10686 (2023).
- [30] A. deMartini, P. Fuentes, R. Orús, P. M. Crespo, and J. E. Martinez, Decoding algorithms for surface codes,

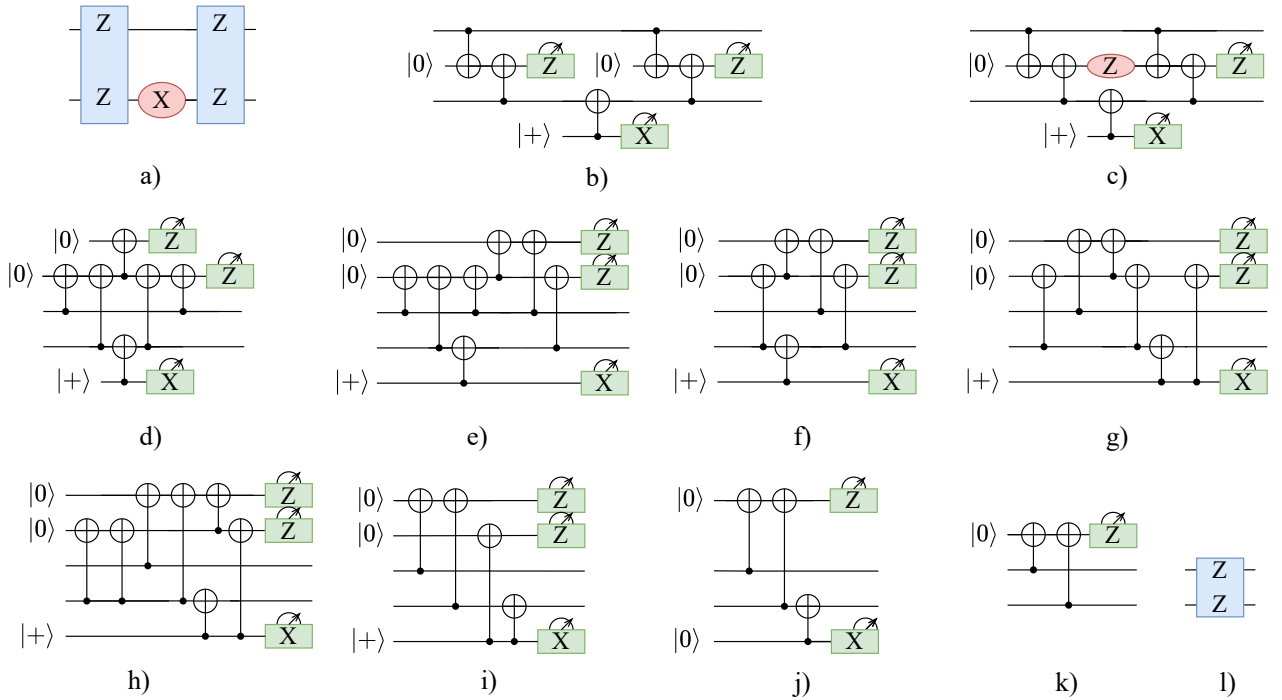


FIG. 10. Correctness of the **FUSE** rewrite rule uses the rewrites listed in Fig. 9 (the figure does not include the corrective terms): a) the start configuration; b) each ZZ interaction is decomposed using **ZZC** and the red X oval is decomposed using the circuit from **MR**; c) applying **MR** between the Z-measurement and the $|0\rangle$ initialization introduces a red Z oval; d) the Z oval is decomposed using the circuit from **MR**; e-i) CNOTs are commuted according to the **CNOT** rule, adjacent CNOTs are cancelled; i) the second ancilla from the top is removed by applying **REMX**; j) the bottom ancilla is removed by applying **REMZ**; k) **ZZC** is applied in the reverse direction; l) end result.

Quantum **8**, 1498 (2024).

- [31] A. G. Fowler, Minimum weight perfect matching of fault-tolerant topological quantum error correction in average $o(1)$ parallel time, arXiv preprint arXiv:1307.1740 (2013).
- [32] D. Poulin, Optimal and efficient decoding of concatenated quantum block codes, Physical Review A—Atomic, Molecular, and Optical Physics **74**, 052333 (2006).
- [33] L. Skoric, D. E. Browne, K. M. Barnes, N. I. Gillespie, and E. T. Campbell, Parallel window decoding enables scalable fault tolerant quantum computation, Nature Communications **14**, 7040 (2023).
- [34] J. T. Anderson, G. Duclos-Cianci, and D. Poulin, Fault-tolerant conversion between the steane and reed-muller quantum codes, Physical review letters **113**, 080501 (2014).
- [35] M. S. Alam and E. Rieffel, Dynamical logical qubits in the bacon-shor code, arXiv preprint arXiv:2403.03291 (2024).
- [36] D. Bacon, Operator quantum error-correcting subsystems for self-correcting quantum memories, Physical Review A—Atomic, Molecular, and Optical Physics **73**, 012340 (2006).
- [37] Y.-C. Zheng, C.-Y. Lai, T. A. Brun, and L.-C. Kwek, Depth reduction for quantum clifford circuits through pauli measurements, arXiv preprint arXiv:1805.12082 (2018).
- [38] B. P. Lanyon, M. Barbieri, M. P. Almeida, T. Jennewein, T. C. Ralph, K. J. Resch, G. J. Pryde, J. L. O’Brien, A. Gilchrist, and A. G. White, Simplifying quantum logic using higher-dimensional hilbert spaces, Nature Physics **5**, 134 (2009).
- [39] Y. Wang, Z. Hu, B. C. Sanders, and S. Kais, Qudits and high-dimensional quantum computing, Frontiers in Physics **8**, 589504 (2020).